Analytical Methods

ROYAL SOCIETY OF CHEMISTRY

PAPER

Cite this: *Anal. Methods*, 2022, **14**, 286

Identification of adducts between oxidized rosmarinic acid and glutathione compounds by electrochemistry, liquid chromatography and mass spectrometry

Emad F. Newair *[a] and François Garcia[b]

Natural polyphenols are omnipresent and are an integral part of the human diet as well as quinones. Glutathione (GSH) is present in a significant amount inside cells and consequently, GSH conjugates of polyphenols will be encountered in the body. In the current work, voltammetry and liquid chromatography–mass spectrometry were carried out to characterize the reaction mechanism of the electrochemical oxidation of polyphenolic rosmarinic acid (RA) with GSH nucleophiles in aqueous solution. Electrochemical investigation of RA revealed that two consecutive transfer steps (which depend on pH) of two electrons and protons occur during the reversible oxidation of RA. Moreover, it was found that the first oxidation step is associated with the 3,4-dihydroxyphenyl lactic acid moiety, whereas the second oxidation step corresponds to the oxidation of the caffeic acid one. By using ultrahigh-performance liquid chromatography-diode array detection-mass spectrometry (UPLC-DAD-MS) in the negative ion mode, the oxidation pathways of RA in the presence of GSH were analyzed, and a total of four RA-GSH conjugates were identified. The oxidative degradation pathway of RA can be better apprehended and forecasted by the acquired results in this study.

Received 5th October 2021
Accepted 9th December 2021

DOI: 10.1039/d1ay01699g

rsc.li/methods

1. Introduction

Food quality can significantly deteriorate *via* an oxidative process which will lead to modifications of safety as well as texture, flavour, and colour of foodstuffs. To prevent food oxidation, polyphenols can play a significant protective role. Among the hydroxycinnamic acid derivative class, rosmarinic acid (RA) is a natural polyphenolic compound that is greatly present in fruits and vegetables for human consumption.[1] Scarpati and Oriente isolated RA from *Rosmarinus officinalis* L. (Lamiaceae) (rosemary) for the first time in 1958,[2] and it is considered to be a constituent of numerous medicinal plant species with one of the highest bioactive effects.[3] It has been reported that RA has many medicinal values, including anti-inflammatory,[4] antiangiogenesis,[5] antioxidant,[6] antitumor,[7] and antiphotodamage properties.[8] A study concerning carnosic and rosmarinic acids, two rosemary components, and their protective effects against oxidative stress as well as hyperlipidemia and hypoglycemia in diabetic rats has been performed.[9] The authors reported that these compounds exhibit a reduction in a significant way of the different levels of triglycerides as well as total cholesterol and fasting plasma glucose. They also reported that, for rats, RA has a more important protective effect concerning symptoms of mitigated diabetes than carnosic acid. Furthermore, other pharmacological activities, notably anti-allergic properties, inhibition of both cyclooxygenase and murine cell proliferation as well as preventive effects on low-density lipoprotein oxidation have been reported.[10]

RA is an ester of caffeic acid (CA) and 3,4-dihydroxyphenyllactic acid (DHPLA) (Fig. 1). Thus, RA can react with free radicals through both catechol moieties (ring A and ring B) it possesses *via* an electron/proton donor mechanism. In addition to that, RA can also easily chelate *via* hydroxyl and carboxyl oxygen.[11] However, despite all these useful therapeutic properties, compounds that contain catechol rings can autoxidize to

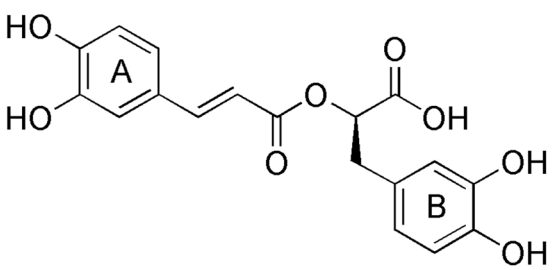

Fig. 1 The chemical structure of RA.

[a]*Unit of Electrochemistry Applications (UEA), Chemistry Department, Faculty of Science, Sohag University, Sohag 82524, Egypt. E-mail: emad.newair@science.sohag.edu.eg*

[b]*SPO, INRA, Montpellier Supagro, Montpellier University, UMR 1083, F-34060, Montpellier, France*

form quinones which accelerate the formation of reactive oxygen species (ROS).[12] The fundament of the biological activity of quinones is based on their capacity to generate oxidative stress with the macromolecules of the cellules. As a result of this stress, damage of molecules needed for cell survival occurs. A quinone is completely reduced by the capture of two electrons and also two protons to a quinol (hydroquinone or catechol). The semiquinone, which is the reduced form of the quinone with only one electron, can react with molecular oxygen with the formation of the superoxide anion radical ($O_2^{\bullet -}$). The $O_2^{\bullet -}$ radical subsequently undergoes either spontaneous or enzyme-catalyzed dismutation to form H_2O_2 (hydrogen peroxide). The superoxide anion radical also reduces Fe^{3+} to Fe^{2+}. Then, hydrogen peroxide can react with Fe^{2+} to produce $OH^{\bullet -}$ (hydroxyl radical). Finally, the quinone-mediated oxidative damage is certainly caused by the $OH^{\bullet -}$ radical. Nucleophilic addition for a quinone corresponds to a formal two-electron reduction. Thus, thiol addition to the quinone double bond corresponds to nucleophilic addition to an α,β-unsaturated carbonyl.[13]

In order to better characterize the preventive role of RA concerning oxidative stress and consequently free radical damage, a study concerning the electrochemical oxidation mechanism of RA appears important. Indeed, the characterization of the antioxidant capacity of polyphenols, as well as the mechanisms of their reactions, can be possible by electrochemical measurements *via* the obtained physicochemical parameters of polyphenols such as the redox potential, the number of transferred electrons during the reaction, the transfer rate constant of electrons, *etc.* These parameters appear to possess great potential not only for evaluating the antioxidant abilities of polyphenols but also for understanding their reaction mechanisms. Some authors investigated electrochemically the rosmarinic acid oxidation in aqueous solutions.[14] They reported that RA was oxidized through an E_rE_r mechanism giving two oxidation–reduction peaks. The electrochemical behavior of rosmarinic acid in phosphate buffer at pH 7.4 was also investigated at the glassy carbon electrode. The electrode reaction mechanism was studied using electrochemical methods, cyclic voltammetry, and square wave stripping voltammetry.[15] Electrochemical studies have showed that the first oxidation step is related to the caffeic acid moiety, whereas the second oxidation step is associated with the oxidation of the 3,4-dihydroxyphenyl lactic acid one.[16] The highest antioxidant potential of RA because of its structural features is higher than those of other hydroxycinnamic acid derivatives.[17–19]

Glutathione which is a natural tripeptide (glutamate, cysteine, and glycine) mainly exists in the reduced form (GSH). It represents the major non-protein sulfhydryl compound in cells.[20] Glutathione reacts with quinones yielding a (2*S*)-glutathionyl product;[21] the reaction of glutathione with quinones is usually estimated to induce a cytoprotective effect. Indeed, nucleophilic sites on macromolecules of cellules with a critical function are preserved from irreversible reactions by the sulfhydryl group of GSH which plays the role of a "sacrificial" nucleophile. Therefore, the use of GSH allows characterization of oxidation products of phenolic compounds. Several biological activities result from the GSH conjugates after the reaction of multiple polyphenolic compounds. Indeed, the redox activity of polyphenols is often increased with GSH conjugation. The distinctive structural features of polyphenolic-GSH conjugates provide the basis concerning structures not only for toxicological activity but also for pharmacological ones.[22] Identification of adducts between RA quinones and thiol compounds was performed using liquid chromatography and mass spectrometry. It was demonstrated that one quinone-RA/GSH adduct was formed.[23] Furthermore, it was reported that several products are obtained by nucleophilic additions on a unique quinone molecule.[24,25]

To better apprehend the prevention of stress induced by oxidation as well as free radical spoilage and particularly concerning natural polyphenols, the electrochemical oxidation mechanism study appears decisive. The antioxidant activity of polyphenols was investigated by numerous electrochemical measurements in the literature.[26–34] We recently investigated the electrochemical oxidation mechanism of eriodictyol with glutathione in aqueous buffer solutions. Pathways of oxidation and characterization of the produced oxidation compounds were studied using electrochemical-ultrahigh-performance liquid chromatography combined with mass spectrometry (EC-UPLC-MS).[35]

In the present article, the oxidation of RA by electrochemical means with GSH in an aqueous solution is studied to investigate the reaction mechanism of the formed RA *o*-quinone intermediate with GSH. The investigation was performed at a GCE using cyclic voltammetry (CV) and square wave voltammetry (SWV). Identification of the oxidation products was elucidated using UPLC-MS. The established electrochemical EC-UPLC-MS exhibits promising performance for the identification of the GSH conjugates of RA.

2. Materials and methods

2.1. Chemical products

Rosmarinic acid (≥97.0%), reduced L-glutathione (≥98.0%), phosphoric acid solution (49–51% HPLC grade), glacial acetic acid (USP reference standard), boric acid (≥99.5% ACS reagent), and sodium hydroxide (≥98% reagent grade) were obtained from Sigma-Aldrich (France). Ethanol (≥99.8% HPLC grade) was purchased from Merck (USA).

2.2. Solution preparation

Britton–Robinson (B–R) buffer was utilized over the pH range from 1.81 to 7.07. Solutions of acetic, boric, and phosphoric acids at a concentration of 0.04 M were prepared. Ammonium hydroxide solution with a concentration of 0.2 M allowed adjusting the pH of the B–R buffer at the desired value using a pH-meter (HI 2210, HANNA, Romania) equipped with a combined pH reference electrode. A concentrated stock solution of rosmarinic acid was prepared at a concentration of 1.05 mM in water/ethanol (50/50 v/v). The solutions were protected from light effect by using aluminium foil and stored at 4 °C. For all experiments, the solutions were prepared freshly by diluting the stock solution. The purified water used in the preparation of all solutions was Milli-Q grade.

2.3. Cyclic and square wave voltammetry

All electrochemical experiments were carried out by means of a potentiostat-galvanostat PGSTAT 128N Autolab (Eco-Chemie, Utrecht, Holland) and the software NOVA 2.0. A three-electrode cell (20 mL) was used, equipped with a glassy carbon working electrode (GCE) (3.0 mm diameter, Metrohm-Autolab, Switzerland), a silver/silver chloride (Ag/AgCl–KCl, 3.0 M) reference electrode, and a platinum wire counter electrode. The surface of the glassy carbon electrode was polished before each measurement using alumina powder (0.3 μm, Metrohm, France), rinsed using Milli-Q water, and finally dipped for 5 minutes in an ultrasonic bath. Then, electrochemical cleaning was carried out by cyclic voltammetry in the Briton–Robinson buffer supporting electrolyte until the steady-state. All measurements were carried out in duplicate.

2.4. Controlled potential electrolysis

The electrolysis experiments were carried out using a coulometric cell (μ-PrepCell, Antec, United States of America) equipped with a rectangular glassy carbon electrode (1.9 cm^2), a HyREF (Pd/H_2) and a titanium electrode as working, reference and auxiliary electrodes, respectively.

In order to study closely the electrochemical oxidation products of rosmarinic acid with or without GSH solution, the electrolysis cell was coupled to an UPLC-MS (Fig. 2). The solution of RA at a concentration of 0.1 mmol L^{-1} in water/ethanol (50/50 v/v) was introduced into the coulometric cell with a 0.1 mL min^{-1} flow rate while a potential of 250 mV (*vs.* Pd/H_2) was continuously applied at the GCE. Until baseline stabilization, the potential was maintained constant for more than 3 minutes. Afterward, the solutions of the oxidized products were sampled under an argon atmosphere in tinted vials in order to be introduced into the UPLC apparatus. In order to trap the oxidation products, a GSH solution at a concentration of 5.0 mmol L^{-1} was utilized.

2.5. UPLC-DAD-MS system

RA and its GSH conjugates have been characterized using UPLC-MS. Analyses were carried out using an Acquity UPLC (Waters, Milford, MA). The detector was a photodiode array (PDA). The column used was a HSS T3, 100 × 2.1 mm, 1.8 mm column, Nucleosil 120-3 C18 end-capped (Macherey-Nagel, Sweden). Concerning the solvents, the following gradient was applied with solvent A (H_2O–HCOOH, 99/1 v/v) and solvent B (CH_3CN–H_2O–HCOOH, 80/19/1 v/v/v): first 0.1% of B; 0 to 5 minutes: linear change to 60% of B; 5 to 7 minutes: to 99% of B; isocratic 99% of B. A mass spectrometer of an AmaZon X electrospray ionization-trap (Bruker Daltonics, Bremen, Germany) was coupled on line with the Acquity UPLC apparatus. The experimental conditions during the analysis were the pressure of the nebulizer 44 psi, the temperature of the dry gas 200 °C with a flow rate of 12 L min^{-1}, and the voltage of the capillary 4 kV. The ionization in the negative mode was used, and the data concerning the mass spectra were followed over a 90–1500 Th mass range. Finally, the speed of the mass spectrum acquisition was set to 8.1 m/z min^{-1}.

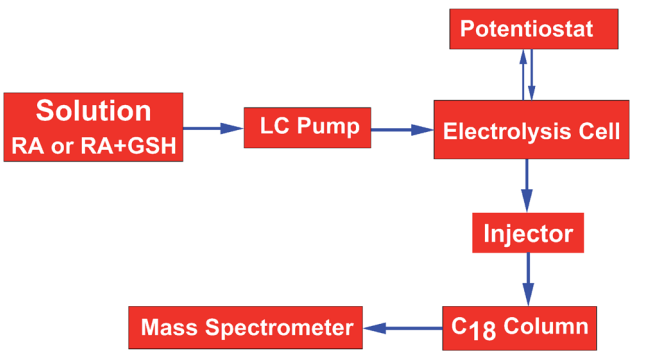

Fig. 2 Schematic presentation of the EC-LC-MS set-up comprising an electrochemical cell (EC), liquid chromatography (LC) and mass spectrometry (MS).

3. Results and discussion

3.1. Electrochemical oxidation behaviour of RA

The electrochemical oxidation behaviour of RA was studied at a GCE using CV and SWV in the pH range between 1.81 and 7.07.

3.1.1. Cyclic voltammetry. The electrochemical behaviour of 25.6 μM RA using CV was investigated on the GCE at different scan rates in Britton–Robinson buffer (pH 2.5) (Fig. 3A). On the positive-going scan, RA exhibits two discernible anodic steps; the first one appears like a shoulder (peak 1_a) for E_{p1a} = +0.449 V whereas the second one appears like a well-defined anodic step (peak 2_a) for E_{p2a} = +0.498 V. On scanning in the negative direction, two cathodic counterpart steps are obtained, a step (peak 2_c) for E_{p2c} = +0.467 V, followed by a step (peak 1_c) for E_{p1c} = +0.420 V. The differences between the anodic and cathodic peak potentials, $\Delta E = (E_{pa} - E_{pc})$ are 29 and 31 mV for the first and the second peaks, respectively, corresponding to a two-electron reversible electrode reaction theoretical value of 30 mV.[36,37] In fact, two catechol moieties are present in the chemical structure of RA, one corresponding to caffeic acid and the other one to DHPLA.

The difference of the oxidation peak potentials for CA and DHPLA is caused by both electron density and inductive effects, considering the electron-withdrawing effect ($-\delta$) of carboxylic and ester groups, opposite to the electron-releasing effect ($+\delta$) of alkyl groups.[27] On one hand, for DHPLA, the carboxyl group causes only a weak negative inductive effect due to the weakening of the electrostatic induction along the chain. On the other hand, for caffeic acid, the carboxyl group maintains the disabling effect caused by the double bond.[38] Nevertheless, the electronic density is diminished, caused by the carboxylic function concerning the phenolic sites. Consequently, the electron transfer will be less straightforward for caffeic acid. Recently, Beiginejad *et al.* performed theoretical studies and their results showed that the two catechol rings of RA oxidized independently of each other. The first redox wave is related to the catechol moiety of DHPLA while the second redox wave is related to the CA moiety.[14] In addition to that, when the scan

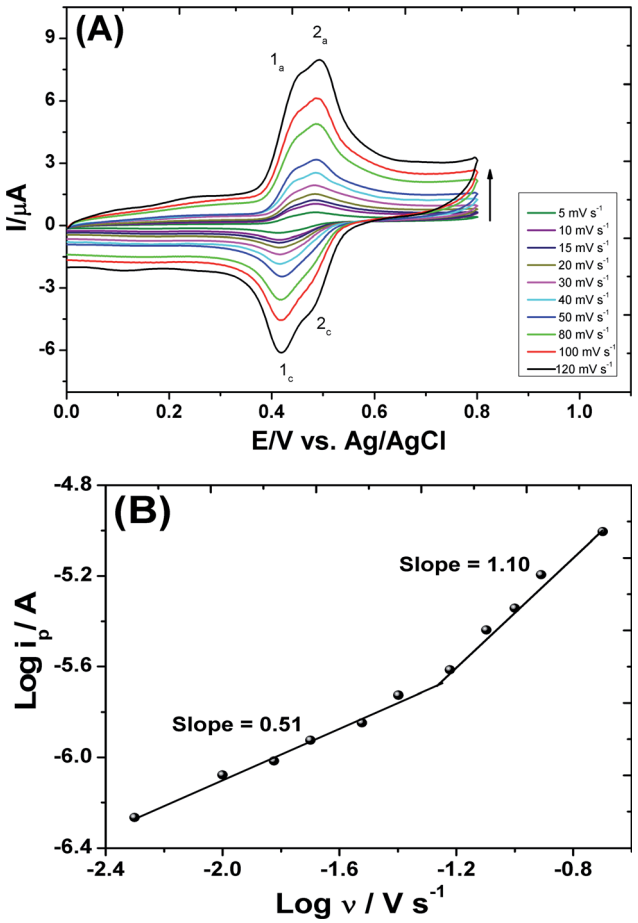

Fig. 3 (A) Cyclic voltammograms of 25.6 μm RA in B–R buffer (pH 2.5) at different scan rates using GCE and (B) log–log relationship.

rate increases, the anodic peak potentials of the two waves are slightly shifted to higher values whereas the cathodic peak potentials of the two waves are slightly shifted to lower values. However, the peak potential difference ΔE remains constant even for important scan rates. Moreover, when the scan rate increases from 5 to 200 mV s^{-1}, a linear log–log variation (log i_p, *vs.* log ν) is obtained with a slope value of 0.51 in the scan rate range from 5 to 60 mV s^{-1} and a slope value of 1.10 in the scan rate range from 80 to 200 mV s^{-1} (Fig. 3B).

Under these experimental conditions, the second step peak current ratio (I_{pc2}/I_{pa2}) is about one, 0.98, at a scan rate of 30 mV s^{-1}: this value can be considered as a stability criterion of the formed RA *o*-quinone at the electrode. Thus, no hydroxylation or dimerization reactions which are slow can be observed during the cyclic voltammetric experiments.[39] On increasing the scan rate, the second step peak current ratio (I_{pc2}/I_{pa2}) and the current function for the second peak ($I_{pa2}/\nu^{1/2}$) are slightly changed. This behaviour is indicative that the electrode reaction follows an $E_{rev}C_{rev}$ mechanism: a reversible electron transfer reaction followed by a reversible chemical reaction.[40] Furthermore, the number of electrons (n) per oxidized molecule is given by Faraday's law of electrolysis (eqn (1)):

$$n = Q/(FN) \quad (1)$$

where Q is the charge passed during electrolysis, F is the Faraday constant and N is the number of moles. Bulk electrolysis was carried out on 2.31×10^{-10} mol of RA in B–R buffer (pH 1.80) at 250 mV *vs.* Pd/H_2 with coulometric analysis. The consumed net charge was 8.69×10^{-5} Coulomb for 2.31×10^{-10} mol of RA which gives 3.9 transferred electrons per molecule considering the global redox process.

The pH effect was studied by performing cyclic voltammograms of 10.40 μM RA on the glassy carbon electrode at 20 mV s^{-1} (scan rate) in Britton–Robinson buffer for different pH values ranging from 1.80 to 7.07 (Fig. 4A). The peak potential (E_p) variation with pH gives worthwhile information concerning the electrode process. Indeed, a shift of the two anodic peak potentials corresponding to smaller positive values occurs when the solution pH is increased. Moreover, it is found that the wave response diminishes until completely disappeared for important pH values (superior to 7.07) (Fig. 4A). This indicates that the concentration of the electroactive form of RA is the highest at acidic pH values, and consequently the concentration of the active RA form is decreased when the solution pH is increased. In addition to that, the formal potential ($E^{\circ\prime}$) can be approximated by the midpoint potential, and a linear decrease of the $E^{\circ\prime}$ value with a slope of −61.0 mV pH^{-1} was obtained plotting

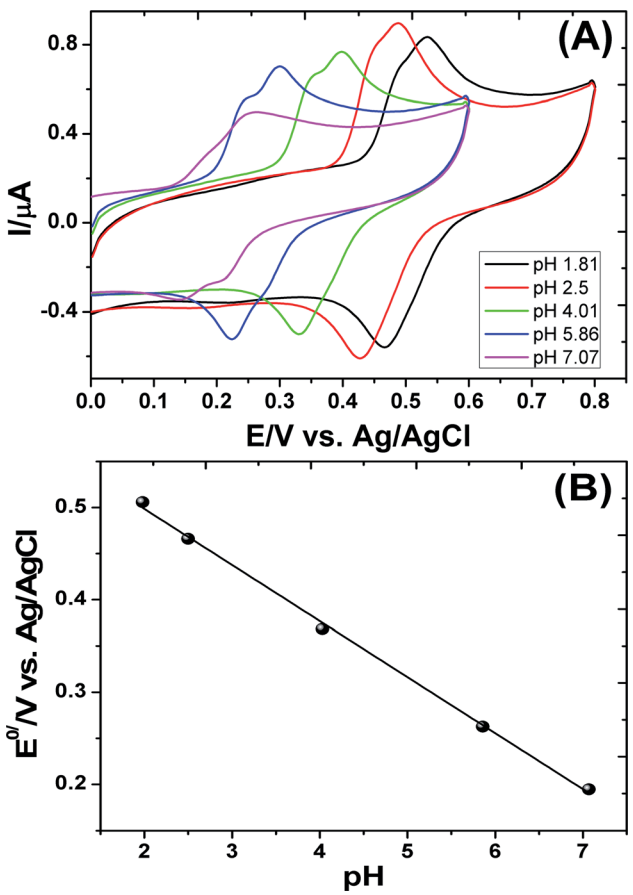

Fig. 4 (A) Cyclic voltammograms of 10.4 μm RA in B–R buffer at different pH values on the GCE at a scan rate of 20 mV s^{-1} (B) E^0/ (midway potential) *vs.* pH relationship.

$E^{\circ\prime}$ as a function of pH (r = 0.988) (Fig. 4B). The obtained relation follows eqn (2):

$$E^{\circ\prime} = E^{\circ} - 2.303(mRT/(nF))\ \mathrm{pH} \quad (2)$$

where m and n are the proton and electron numbers in the redox reaction, respectively, R is the gas constant and T is the absolute temperature. The intercept at pH = 0 gives the standard redox potential E° (0.620 V). The slope of the straight line is close to the expected value for a system with an equal number of electrons and protons. Thus, the overall anodic oxidation of RA under such conditions is a reversible oxidation of the two catechol groups involving both two electrons and two protons to the corresponding *o*-quinone. It worth noting that ring A conjugated to a double bond connected with a carbonyl group which increases the reversibility of the electrode reaction. This enhances the electron delocalization resonance effect from the aromatic nucleus to the formed phenoxyl radicals which leads to phenoxy stabilization.

3.1.2. Square wave voltammetry. The behaviour of the square wave voltammetric experiments of 1.0 μM RA in Britton–Robinson buffer (pH 2.5) for pulse amplitude 25 mV, frequency 12 Hz and step potential 1 mV was investigated at the GCE (Fig. 5). RA shows two anodic waves, the first one appears (peak 1_a) at a net peak potential (ΔE_{p1}) of 434 mV, followed by the second one (peak 2_a) at a ΔE_{p2} of 490 mV. The forward current (oxidation process), the backward current (reduction process) and the resultant net current are illustrated in Fig. 5A. This clearly indicates that the electrode process of RA is a reversible oxidation process. Besides, concerning the components of wave 1_a, the forward peak current (I_{1f}) is higher than the backward one (I_{1b}) with a current ratio (I_{1f}/I_{1b}) equal to 1.06. This behavior indicates that the electrode reaction is coupled with partial adsorption of the reactant on the surface of the electrode.

Additionally, multi-scan SW voltammograms without cleaning the electrode show that the net peak current (ΔI_{1a}) after the first scan tends to decrease (Fig. 5B). On subsequent potential cycling, the response (ΔI_{1a}) is further decreased and the developed peak response increases. This finding is evidence of the adsorption of the generated RA oxidation product on the surface of the electrode during the cycling. On increasing the frequency, RA shows an anodic shoulder peak (peak 1_a) followed by a second anodic peak (peak 2_a) (Fig. 6A). Furthermore, the peak potential is slightly changed, and the net peak current ($\Delta 2i_a$) is gradually changed. It was found that ($\Delta 2i_a$) varied with frequency. Moreover, a linear relation is obtained between $\log(\Delta 2i_a)$ *vs.* $\log f$ with a value of 0.71 for the slope (Fig. 6B). This reveals that the oxidation of RA is a diffusion-controlled process coupled with some adsorption. Furthermore, the peak potential ΔE_{p2} is independent of the log frequency over the entire range of investigation, indicating that both oxidized and reduced forms of RA are confined to the electrode surface.[41] This confirms the proposed mechanism obtained from the cyclic voltammetric behaviour of RA. The variation of the SW peak potentials *versus* the frequency logarithm is not linear (data not shown). This behavior is attributed to a reversible redox system controlled by

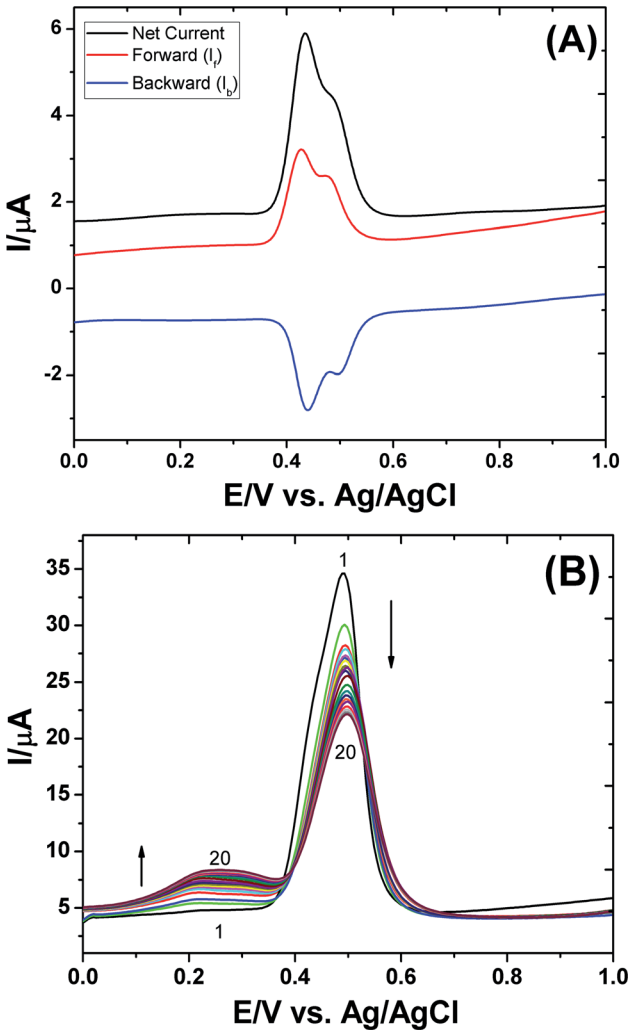

Fig. 5 (A) SWV of 1.0 μm RA in B–R buffer (pH 2.5) at the GCE: pulse amplitude 25 mV, frequency 12 Hz and step potential 1 mV. (B) SWV of 25.6 μm RA in B–R buffer (pH 2.5) by applying several repetitive scans on the GCE without cleaning the electrode: frequency 20 Hz, pulse amplitude 25 mV and step potential 1 mV.

adsorption of the reactant.[42] Furthermore, the SW current peak ($\Delta 2i_a$) increases proportionally to the SW amplitude for $a \leq 60$ (data not shown). This response is attributed to the reversible redox reaction of RA controlled by the adsorption process. Fig. 7 shows the influence of the RA concentration on the square wave voltammograms for a frequency of 12 Hz and a pH of 2.5. Whatever the studied concentration (1.0 to 24.4 μM), the SW voltammograms show two separate peaks. The first peak corresponds to the catechol moiety of DHPLA whereas the second peak is related to the oxidation of the CA one, as discussed previously. The dependence of the net peak current on the RA concentrations is sigmoidal (inset of Fig. 7). It is worth mentioning that the inset of Fig. 7 is plotted using the net peak current ($\Delta 2i_a$) of the two oxidation peaks. The inset of the figure shows that up to the concentration of 4.5 μM, the relationship between the current and concentration is linear. After this concentration, the relationship is no longer linear and the

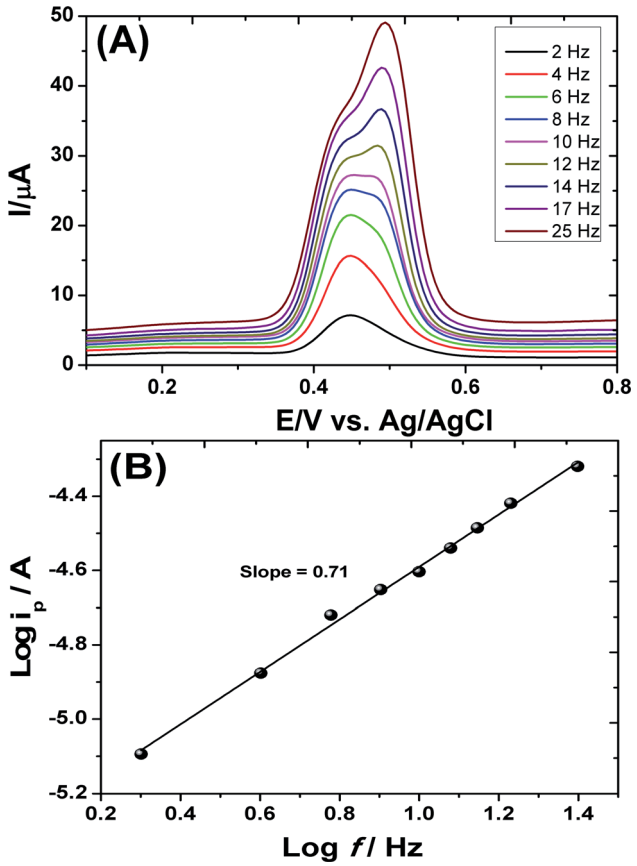

Fig. 6 Square wave voltammograms of 25.6 μm RA in B–R buffer (pH 2.5) at the GCE (A) at different SW frequencies at pulse amplitude 25 mV and step potential 1 mV, and the (B) log–log relationship.

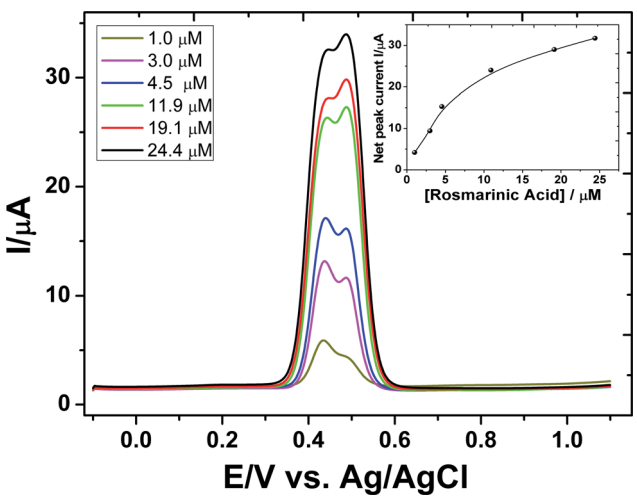

Fig. 7 SW voltammograms of RA at different concentrations in the range from 1.0 to 24.4 μm: pulse amplitude 25 mV, frequency 12 Hz and step potential 1 mV. The inset is the ($\Delta 2i_a$)–[RA] relation.

electrode surface becomes saturated at high concentrations. These results provide additional proof that, under these experimental conditions, the overall electrode process shows diffusion/adsorption mixed control.

3.2. Cyclic voltammetry of RA with GSH

Electrochemical behaviour of 21.0 μM RA was investigated by cyclic voltammetry at a scan rate of 20 mV s^{-1} on a GCE in Britton–Robinson buffer solution (pH 1.80 and 4.9) for GSH concentrations varying from 0.074 to 0.614 mM. The obtained CV responses are presented in Fig. 8A. With addition of GSH to RA, the voltammograms present a slight increase in the main anodic peak current (I_{2a}) jointly with low more positive potentials while a large decrease in the cathodic counterpart peak current (I_{2c}) occurs with low peak potentials shifting to less positive values. On the other hand, at pH 4.9, RA shows a significant change and the voltammogram exhibits an irreversible feature, a remarkable improvement of the anodic peak current with intense reduction of the cathodic peak current by increasing the GSH content (Fig. 8B). This indicates that an electrocatalytic reaction occurs; RA undergoes electrochemical oxidation to form RA *o*-quinone, which in turn rapidly reacts with GSH to regenerate back RA and converts GSH to disulfide GSSG.

Fig. 8C shows the peak current ratio (Ip^c/I_p^a) *versus* the GSH concentration with a diminution of the peak current ratio value at pH 1.80 while at pH 4.9, the ratio changes significantly, and therefore the cathodic counterpart disappears. Thus, it is revealed that the chemical reaction rate of the interaction of GSH with the *o*-quinone depends on its concentration. When the GSH concentration is weak, only a low nucleophilic attack of GSH on the electro-produced *o*-quinone occurs. In contrast, on increasing the GSH contents, the nucleophilic attack of GSH on the *o*-quinone increases. The lowering of the cathodic peak current (or its disappearance) is ascribed to the existence of a fast subsequent nucleophilic reaction between GSH and the electro-produced RA *o*-quinone. The nucleophilic attack of GSH on the *o*-quinone reduces the *o*-quinone content in the reaction layer; consequently, the cathodic peak current will be reduced or totally disappears. It is thus suggested that the oxidation mechanism of RA when GSH is present in solution follows an $E_{rev}C_{irr}$ mechanism for which RA was initially oxidized to form RA *o*-quinone at ~440 mV through a reversible electron-transfer step (E_{rev}). Then, the quinone species oxidizes GSH through an irreversible catalytic chemical reaction (C_{irr}) to give glutathione disulfide GSSG and the original RA at 440 mV, and GSH can also be oxidized in the vicinity of this potential. Two possible electrochemical reaction pathways are proposed as shown in Scheme 1. In the first reaction pathway, GSH undergoes a homogeneous catalytic reduction by RA *o*-quinone to give the parent RA and generates the disulfide (GSSG) (pathway 1). In the second reaction pathway, the GSH conjugate of RA is produced on the reaction of GSH with the generated RA *o*-quinone (pathway 2). The generation of phenolic compounds (the parent RA and its GSH conjugates) which are further oxidized at the GCE is the overall process of both pathways. The observed anodic peak current enhancement and the decrease of the cathodic counterpart intensity of RA when GSH is present in solution as illustrated in Fig. 8 are due to the formation of new phenolic compounds. Furthermore, the total irreversibility of the cyclic

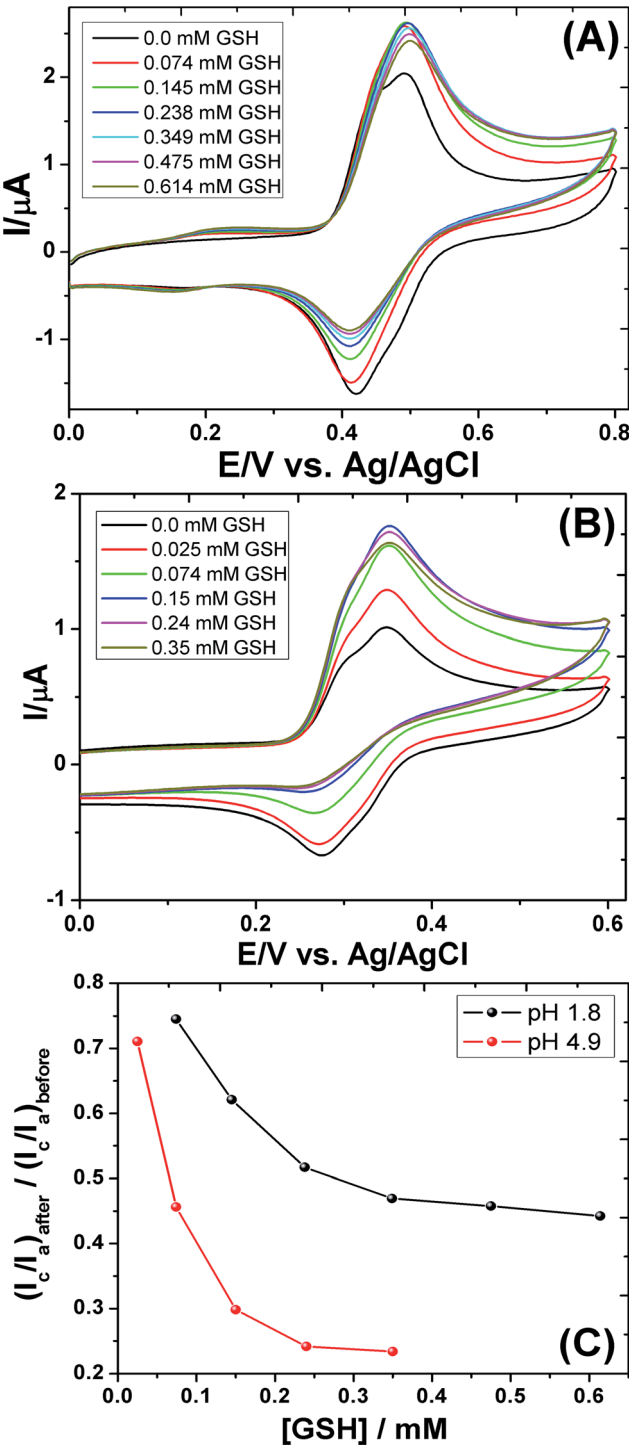

Fig. 8 Influence of GSH on the cyclic voltammograms of 21.0 μm RA on the GCE in Britton–Robinson buffer at a scan rate of 20 mV s^{-1} at (A) pH 1.80 and (B) pH 4.90, and (C) ratio of the cathodic to anodic peak current before and after GSH addition at different pH values.

voltammograms for important GSH concentrations undoubtedly indicates the easy and quick interaction between the electroformed RA *o*-quinone and GSH, and no RA is present to cause reduction at the surface of the electrode during the scan in the reverse way. Therein, the diminution of the ratio of the current ratio I_{pc}/I_{pa} was taken to indicate the interaction degree between *o*-quinone and GSH (Fig. 8C). Obviously, the increase of the midpoint ($E^{\circ\prime}$) value implies that RA tends to be stabilized and protected against oxidation by GSH for high pH values, as established before with the catechol reaction with GSH.[42,43]

3.3. Identification of RA oxidation products by UPLC-MS

At pH 1.8, RA was electrochemically oxidized with GSH in solution by means of a coulometric cell coupled with liquid chromatography-mass spectrometry by two methods. First, in order to avoid the direct oxidation of GSH in the electrochemical cell, RA was firstly oxidized and then collected in GSH solution (0.5 mM) (approach 1). Secondly, both RA and GSH in excess (0.5 mM) were introduced into the coulometric cell, and the oxidation products were collected (approach 2). UPLC-MS analysis showed that an important part of GSH remained reduced after the electrolysis, thus reacting with the quinonic forms although there is a possibility of the oxidation of GSH at a potential of 250 mV (*vs.* Pd/H_2) at the electrolysis electrode. Important quantities of adducts were obtained by the two studied approaches. When the solution was electrolyzed at a maintained potential of 0 mV (*vs.* Pd/H_2), only *m*/*z* 359 $[M - H]^-$ was detected, assigned to RA (Fig. 9, peak A), illustrating that no substantial oxidation of RA in the electrochemical cell occurs. However, electrolysis at a higher potential of 250 mV (*vs.* Pd/H_2) allows the production of new compounds (Fig. 9) after trapping with glutathione at the exit of the electrochemical cell (approach 1). The observed peaks at *m*/*z* 664 $[M - H]^-$ (peak B) and *m*/*z* 969 $[M - H]^-$ (peak C) corresponded to the mono- and bi-GSH conjugates of RA, respectively. As illustrated in Fig. 9, the presence of RA (peak A) as a significant peak shows that it is still in the reduced form after electrolysis, probably resulting from the fact that RA *o*-quinone is reduced back to RA by GSH, as illustrated in Scheme 1 in pathway 1. For the second method (approach 2), oxidation by applying a potential of 250 mV (*vs.* Pd/H_2) on RA and GSH solution for 5 minutes generates new peaks in the UPLC chromatogram at 330 nm (Fig. 9, red curve: peaks D and E). Peak D at *m*/*z* 637 $[M - 2H]^{2-}$ and peak E at *m*/*z* 789 $[M - 2H]^{2-}$ corresponded to the mass of tri- and four-GSH conjugates of RA, respectively. Moreover, the UPLC chromatogram shows, close to these characteristic peaks, numerous peaks around signals B and E corresponding to the identical compound and possessing an identical mass. The explanation can probably come from the existence of stereoisomers which can be separated by the column inducing two or more peaks with the same spectra. Distinctions of arrangement can explain that the isomeric connections have identical spectra although they have distinct retention times. Thus, notable modifications of the phase affinity interaction with the column can occur, bringing a slow-down of the isomer with identical mass.[44] In this regard, the production of tri- and four-GSH conjugates seems to be favoured by the electrochemical oxidation of RA with GSH in solution. Consequently, Schemes 2 and 3 summarize the electrochemical oxidation pathways of RA.

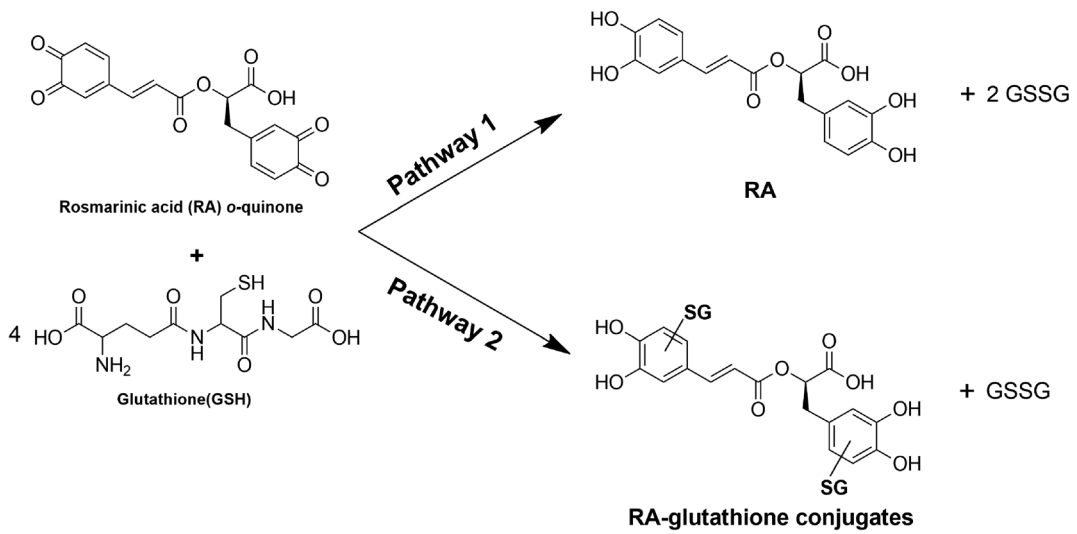

Scheme 1 Possible oxidation pathways of the reaction between RA and GSH.

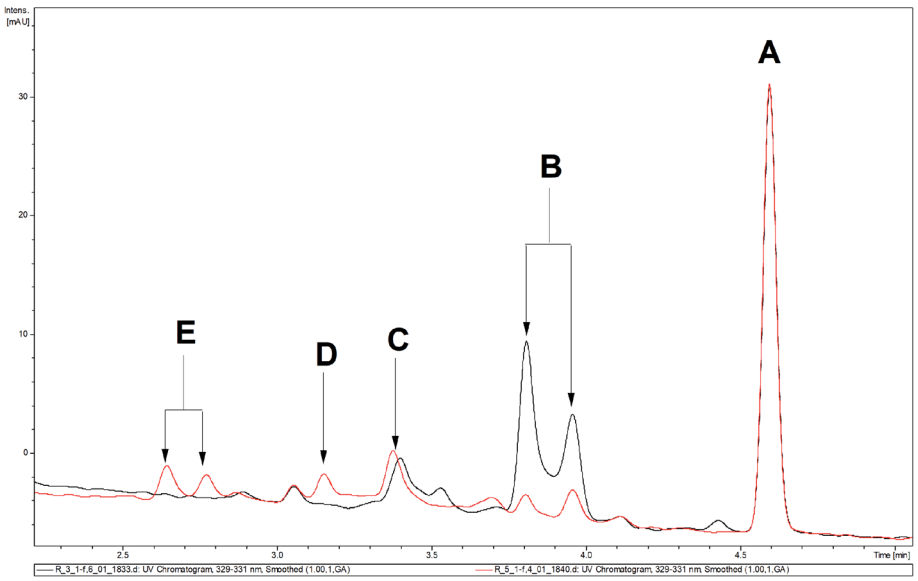

Fig. 9 UPLC chromatograms at 330 nm of a 21.0 μm RA solution (pH 1.8) oxidized at 250 mV *vs.* Pd/H_2 and trapped by a 0.5 mm GSH solution (black curve) and a 21.0 μm RA solution oxidized at 250 mV *vs.* Pd/H_2 in the presence of 0.5 mm GSH solution (red curve).

Considering all the previous results, it can be concluded that the *o*-quinone intermediate is formed during the electrochemical oxidation of RA and its conversion into the GSH conjugates of RA is easily affected. The mass spectrometry analysis (Fig. 10) revealed that numerous RA conjugates are formed during the electrochemical oxidation: mono-, bi-, tri- and four-GSH conjugates of RA, which corresponded to the observed signals at *m*/*z* 664 $[M - H]^-$ (B); 969 $[M - H]^-$ (C); 637 $[M - 2H]^{2-}$ (D) and 789 $[M - 2H]^{2-}$ (E), respectively. GSH can attack the produced *o*-quinone in positions as illustrated in Fig. 11. It concerns not only the reactive centres at C5 and C2 positions of the phenolic ring near the carbonyl groups relative to the *o*-quinone moiety but also the center at the C6 position which is the least good electrophile. In balance with electrophilic behaviour, steric hindrance plays a crucial role in the distinguishing factor of the reaction of GSH on electrophilic centres and it increases in the order C5 < C6 < C2. Thus, although the C2 center is more electrophilic than the C6 center, the latter is more easily attacked by glutathione. Given all these considerations, the mono-GSH conjugate will be preferentially formed at the C5 site since it presents the least steric hindrance as well as the more important electrophilic character.[45] In addition to that, the second attack of glutathione certainly occurs on the C2 site rather than on the C6 center although these two sites are available. Indeed, the C2 center is, in comparison, a less crowded position rather than the other GSH

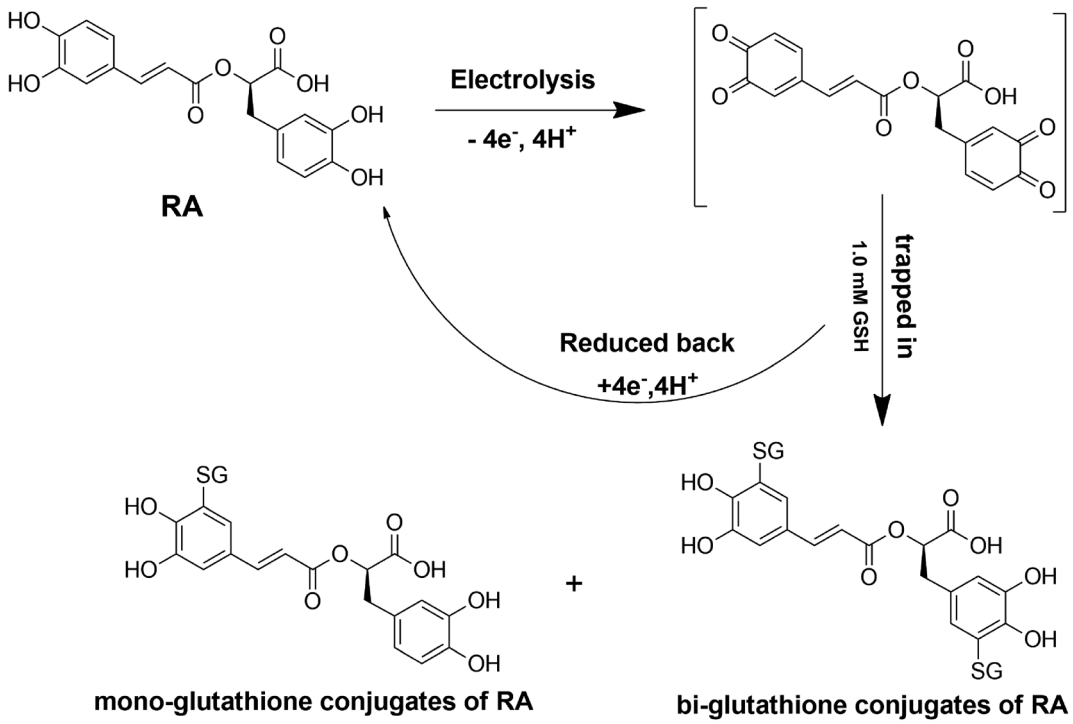

Scheme 2 Proposed pathways of the electrochemical oxidation of RA and trapping of the oxidized products in GSH solution.

conjugate of rosmarinic acid, and the combination of both C6 and C5 sites is not favourable. Therefore, nucleophiles like GSH easily react with oxidized RA, and the *o*-quinone is a highly reactive species, explaining the cellular defence role played by GSH against reactive quinones.[46] Consequently, as illustrated in Fig. 9 and 10, the mono-, bi-, tri- and four-GSH conjugates of RA lead to the existence of the intermediate radical species by the abstraction of one electron-one proton to the catechol moiety of

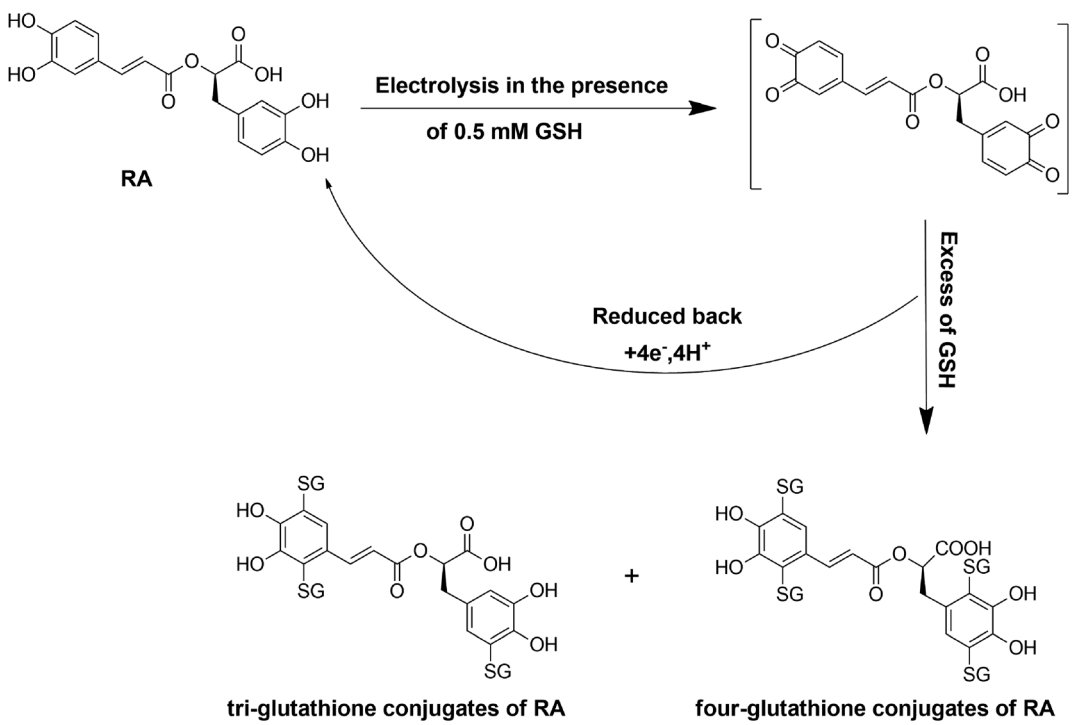

Scheme 3 Mechanistic pathways of the electrochemical oxidation of RA in the presence of GSH.

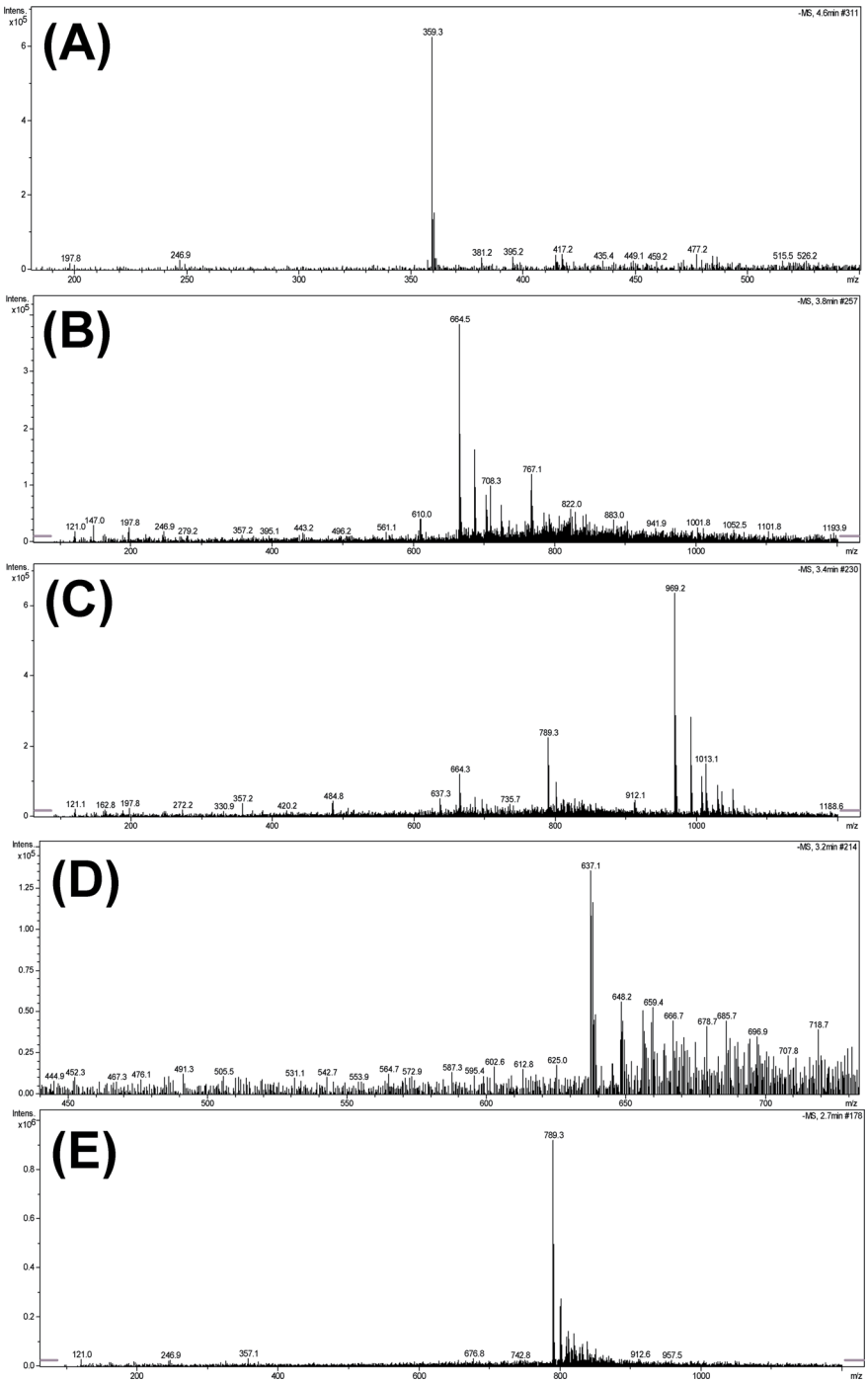

Fig. 10 Negative ion mass spectra of a 21.0 μm RA solution oxidized at 250 mV *vs.* Pd/H_2 in the presence of a 0.5 mm GSH solution (pH 1.8). (A) Signal at *m*/*z* 359 $[M - H]^-$ corresponds to RA; (B) signal at *m*/*z* 664 $[M - H]^-$ corresponds to mono-glutathione conjugates of RA; (C) signal at *m*/*z* 969 $[M - H]^-$ corresponds to bi-glutathione conjugates of RA; (D) signal at *m*/*z* 637 $[M - 2H]^{2-}$ corresponds to tri-glutathione conjugates of RA and (E) signal at *m*/*z* 789 $[M - 2H]^{2-}$ corresponds to four-glutathione conjugates of RA.

RA. After another one electron-one proton, the quinone will be formed from the radical intermediate. The high nucleophilicity of GSH allows it to react with numerous species such as quinones in order to produce GSH-adducts. Thus, the mechanistic study of electrochemical oxidation of RA leads to the pathways proposed in Schemes 2 and 3. When the oxidation products of the electrochemical oxidation of RA are trapped in GSH solution, mono- and bi-GSH conjugates of RA are formed (Scheme 2). In contrast, more GSH adducts are generated when the oxidation of RA occurs in the presence of GSH in the electrochemical cell (Scheme 3).

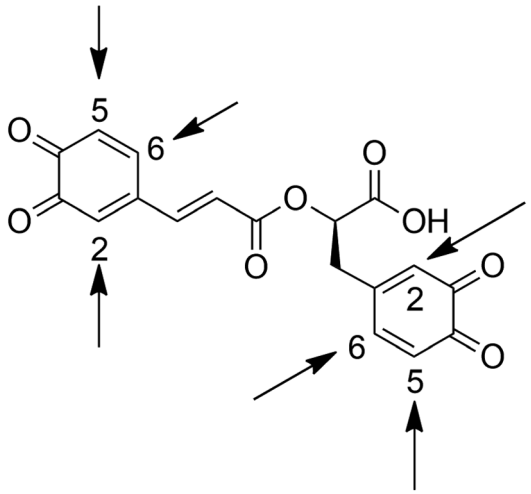

Rosmarinic acid (RA) *o*-quinone

Fig. 11 Pattern for the GSH conjugate formation of RA.

4. Conclusions

The combination of electrochemical approaches with ultrahigh-performance liquid chromatography-mass spectroscopy (EC-UPLC-MS) is a worthwhile technique for identifying the oxidation products of rosmarinic acid and glutathione that are often very complicated to identify. In the current study, we have successfully implemented such a combined system for investigating the behaviour of rosmarinic acid and elucidating the oxidation mechanism in the absence and the presence of glutathione in aqueous solutions. Catechol moieties of rosmarinic acid are easily oxidized to form reactive *o*-quinones which can form adducts with glutathione, including mono-, bi-, tri- and tetra-glutathione conjugates of rosmarinic acid. The chemical structure of the electrochemically generated adducts was confirmed by using liquid chromatography coupled with mass spectroscopy. The obtained results clearly confirm that EC-UPLC-MS exhibits significant potential to investigate/identify the oxidation behaviour of RA.

Author contributions

The following statement illustrates the individual contributions of each author. E. F. N. and F. G. have set up the conceptualization, while E. F. N. has performed the methodology, software analysis, validation, formal analysis, investigation, and data curation. E. F. N. has written the original draft preparation, while F. G. has performed the writing – review and editing.

Conflicts of interest

The authors declare that there is no conflict of interest to publish this paper.

Acknowledgements

The authors appreciate the financial support from the Egyptian Ministry of Higher Education and Scientific Research, Science and Technology Development Fund (STDF) (Grant No. 5361), Egypt. The authors also acknowledge SPO, INRA, Montpellier Supagro, Montpellier University, France.

References

1 S. U. Park, M. R. Uddin, H. Xu, Y. K. Kim and S. Y. Lee, *Afr. J. Biotechnol.*, 2008, **7**, 4959.
2 M. L. Scarpati and G. Oriente, Isolamento e costituzione dell'acido rosmarinico (*dal Rosmarinus off.*), *Ric. Sci.*, 1958, **28**, 2329.
3 M. Petersen, Y. Abdullah, J. Benner, D. Eberle, K. Gehlen, S. Hücherig, V. Janiak, K. H. Kim, M. Sander, C. Weitzel and S. Wolters, *Phytochemistry*, 2009, **70**, 1663.
4 D. de Sá Coutinho, M. T. Pacheco, R. L. Frozza and A. Bernardi, *Int. J. Mol. Sci.*, 2018, **19**, 1812.
5 S. S. Huang and R. L. Zheng, *Cancer Lett.*, 2006, **239**, 271.
6 O. Fadel, K. ElKirat and S. Morandat, *Biochim. Biophys. Acta*, 2011, **1808**, 2973.
7 R. Sharmila and S. Manoharan, *Indian J. Exp. Biol.*, 2012, **50**, 187.
8 M. Sanchez-Campillo, J. A. Gabaldon, J. Castillo, O. Benavente-Garcia, M. J. Del Bano, M. Alcaraz, V. Vicente, N. Alvarez and J. A. Lozano, *Food Chem. Toxicol.*, 2009, **47**, 386.
9 J. Ou, J. Huang, D. Zhao, B. Du and M. Wang, *Food Funct.*, 2018, **9**, 851.
10 D. H. Park, S. J. Park, J. M. Kim, W. Y. Jung and J. H. Ryu, *Fitoterapia*, 2010, **81**, 644.
11 J. Psotová, J. Lasovsk and J. Viar, *Biomed. Pap.*, 2003, **147**, 147.
12 A. Yamanaka, O. Oda and S. Nagao, *FEBS Lett.*, 1997, **401**, 230.
13 L. Jeftic and G. Manning, *J. Electroanal. Chem.*, 1970, **26**, 195.
14 H. Beiginejad, M. Moradi, S. Paziresh and H. Farahani, *J. Electrochem. Soc.*, 2018, **165**, H698–H704.
15 J. Wang, K. Zhang, J. Zhou, J. Liu and B. Ye, *Sens. Lett.*, 2013, **11**, 305.
16 S. Gil Ede, T. A. Enache and A. M. Oliveira-Brett, *Comb. Chem. High Throughput Screening*, 2013, **16**, 92.
17 S. Chen, Y. Fu and R. Wu, *Acta Pharmacol. Sin.*, 1999, **34**, 881.
18 J. L. Lamaison, C. Petitjean-Freytet and A. Carnat, *Pharm. Acta Helv.*, 1991, **66**, 185.
19 J. L. Lamaison, C. Petitjean-Freytet, F. Duband and A. A. Carnat, *Fitoterapia*, 1991, **62**, 166.
20 N. Taniguchi, T. Higashi, Y. Sakamoto and A. Meister, *Glutathione Centennial: Molecular Perspectives and Clinical Implications*, Academic Press, San Diego, CA, 1989.
21 F. Sonni, A. C. Clark, P. D. Prenzler, C. Riponi and G. R. Scollary, *J. Agric. Food Chem.*, 2011, **59**, 3940.
22 T. J. Monks and S. S. Lau, *Chem. Res. Toxicol.*, 1997, **10**, 1296.
23 C. B. Tang, W. G. Zhang, C. Dai, H. X. Li, X. L. Xu and G. H. Zhou, *J. Agric. Food Chem.*, 2015, **63**, 902.

24 S. S. Lau, B. Hill, R. J. Highet and T. J. Monks, *Mol. Pharmacol.*, 1988, **34**, 829.
25 K. G. Eckert, P. Eyer, J. Somenbichler and I. Zetl, *Xenobiotica*, 1990, **20**, 351.
26 M. N. Peyrat-Maillard, S. Bonnely and C. Berset, *Talanta*, 2000, **51**, 709.
27 M. Born, P. A. Carrupt, R. Zini, F. Bree, J. P. Tillement, K. Hostettmann and B. Testa, *Helv. Chim. Acta*, 1996, **79**, 1147.
28 S. A. B. E. van Acker, D. J. van den Berg, M. N. J. L. Tromp, D. H. Griffioen, W. P. van Bennekom, W. J. F. van der Vijgh and A. Bast, *Free Radical Biol. Med.*, 1996, **20**, 331.
29 B. Yang, A. Kotani, K. Arai and F. Kusu, *Anal. Sci.*, 2001, **17**, 599.
30 H. P. Hendrickson, M. Sahafayen, M. A. Bell, A. D. Kaufman, M. E. Hadwiger and C. E. Lunte, *J. Pharm. Biomed. Anal.*, 1994, **12**, 335.
31 L. V. Jørgensen and L. H. Skibsted, *Free Radical Res.*, 1998, **28**, 335.
32 S. Chevion, M. A. Roberts and M. Chevion, *Free Radical Biol. Med.*, 2000, **28**, 860.
33 S. Chevion, E. M. Berry, N. Kitrossky and R. Kohen, *Free Radical Biol. Med.*, 1997, **22**, 411.
34 S. Mannino, O. Brenna, S. Buratti and M. S. Cosio, *Electroanalysis*, 1998, **10**, 908.
35 E. F. Newair, A. Nafady, R. Abdel-Hamid, A. M. Al-Enizi and F. Garcia, *Electroanalysis*, 2018, **30**, 1706.
36 R. Petrucci, P. Astolfi, L. Greci, O. Firuzi, L. Saso and G. Marrosu, *Electrochim. Acta*, 2007, **52**, 2461.
37 M. Salas-Reyes, J. Hernández, Z. Domínguez, F. J. González, P. D. Astudillo, R. E. Navarro, E. Martínez-Benavidez, C. Velázquez-Contrerase and S. Cruz-Sánchez, *J. Braz. Chem. Soc.*, 2011, **22**, 693.
38 E. S. Gil, C. H. Andrade, N. L. Barbosa, R. C. Braga and S. H. P. Serrano, *J. Braz. Chem. Soc.*, 2012, **23**, 565.
39 A. Fakhari, S. Hosseiny Davarani, H. Ahmar and S. Makarem, *J. Appl. Electrochem.*, 2008, **38**, 1743.
40 R. S. Nicholson and I. Shain, *Anal. Chem.*, 1964, **36**, 706.
41 M. Lovrić and Š. Komorsky-Lovric, *J. Electroanal. Chem. Interfacial Electrochem.*, 1988, **248**, 239.
42 P. T. Lee, D. Lowinsohn and R. G. Compton, *Analyst*, 2014, **139**, 3755.
43 P. T. Lee, K. R. Ward, K. Tschulik, G. Chapman and R. G. Compton, *Electroanalysis*, 2014, **26**, 366.
44 J. J. Pitt, *Clin. Biochem. Rev.*, 2009, **30**, 19.
45 M. Y. Moridani, H. Scobie, A. Jamshidzadeh, P. Salehi and P. J. O'Brien, *Drug Metab. Dispos.*, 2001, **29**, 1432.
46 P. J. O'Brien, *Chem.-Biol. Interact.*, 1991, **80**, 1.